



HAL
open science

OPA1 alternate splicing uncouples an evolutionary conserved function in mitochondrial fusion from a vertebrate restricted function in apoptosis.

Aurélien Olichon, Ghizlane Elachouri, Laurent Baricault, Cécile Delettre,
Pascale Belenguer, Guy Lenaers

► **To cite this version:**

Aurélien Olichon, Ghizlane Elachouri, Laurent Baricault, Cécile Delettre, Pascale Belenguer, et al.. OPA1 alternate splicing uncouples an evolutionary conserved function in mitochondrial fusion from a vertebrate restricted function in apoptosis.: OPA1 isoforms in mitochondrial fusion or apoptosis.. Cell Death and Differentiation, 2007, 14 (4), pp.682-92. 10.1038/sj.cdd.4402048 . inserm-00164127

HAL Id: inserm-00164127

<https://inserm.hal.science/inserm-00164127>

Submitted on 6 Mar 2008

HAL is a multi-disciplinary open access archive for the deposit and dissemination of scientific research documents, whether they are published or not. The documents may come from teaching and research institutions in France or abroad, or from public or private research centers.

L'archive ouverte pluridisciplinaire **HAL**, est destinée au dépôt et à la diffusion de documents scientifiques de niveau recherche, publiés ou non, émanant des établissements d'enseignement et de recherche français ou étrangers, des laboratoires publics ou privés.

OPA1 alternate splicing uncouples an evolutionary conserved function in mitochondrial fusion from a vertebrate restricted function in apoptosis.

Running title: OPA1 isoforms in mitochondrial fusion or apoptosis.

Aurélien Olichon^{1,3}, Laurent Baricault¹, Pascale Belenguer¹ and Guy Lenaers^{1,2,4}.

(1) : Laboratoire de Biologie Cellulaire et Moléculaire du Contrôle de la Prolifération, UMR 5088, Université Paul Sabatier, 118 route de Narbonne, 31062 Toulouse cedex 04.

(2) : INSERM U583, Institut des Neurosciences de Montpellier. BP 74103.
34091 MONTPELLIER cedex 5

(3) : Present address : EMBL, Meyerhofstrasse 1, 69117 Heidelberg, Germany.

(4) : To whom correspondance should be addressed : glen@montp.inserm.fr

Tel: (33/0) 499 63 60 53 Fax: (499 63 60 20)

ABSTRACT:

Mitochondrial outer and inner membrane dynamics are key processes in the switch from growth conditions to cell death. During apoptosis, fission of the mitochondrial network and drastic remodelling of the cristae structures occur, and involve the intramitochondrial dynamin OPA1. The 8 possible OPA1 isoforms result from the alternate splicing combinations of exons 4, 4b and 5b. We show here that exon 4, which is conserved throughout evolution, confers functions to OPA1, involved in the maintenance of the $\Delta\Psi_m$ and in the fusion of the mitochondrial network. Conversely, exon 4b and exon 5b, that are vertebrate specific, define a function involved in cytochrome c release, an apoptotic process also restricted to vertebrates. The uncoupling of OPA1 functions confirms that nuclear splicing can control mitochondrial dynamic fate and susceptibility to pathologies.

Key words: OPA1, alternate splicing, mitochondria, fusion, apoptosis,

Abbreviations list:

<i>cyt c</i> :	cytochrome c
OMM:	outer mitochondrial membrane
IMM:	inner mitochondrial membrane
IMS:	inter membrane space
$\Delta\Psi_m$:	mitochondrial membrane potential
IF:	immuno-fluorescence
TEM:	transmission electron microscopy
ADOA:	autosomal dominant optic atrophy

INTRODUCTION:

Mitochondrial membrane dynamics, involving both the fusion-fission of the mitochondrial network and remodelling of cristae structures are essential processes in cellular adaptation to changes of growth conditions and programmed cell death (1; 2). Both the outer and inner mitochondrial membrane (OMM and IMM) dynamics involve large GTPases: respectively the Mitofusins, MFN1 and MFN2 (3; 4), and the dynamin-related protein, DRP1 (5) on the OMM, and the dynamin related OPA1, localized in the inter membrane space (IMS) (6). Mitochondrial fission can be activated by the apoptotic machinery, and physical and functional interactions between apoptotic proteins including Bcl2-homolog domains and DRP1 and Mitofusins have been identified (7-9). Further regulation of the equilibrium between fission and fusion is associated to the IMM potential ($\Delta\Psi_m$) (10) and the IMM structural integrity (11). The IMM forms an architecturally complex structure which has been reconsidered recently in the light of tomography analysis associated to transmission electron microscopy (TEM). Indeed, tubular inner membrane junctions, called cristae junctions, have been evidenced between the IMM facing the OMM, and the vesicular shaped cristae (12). In vertebrate cells, during apoptosis, the cristae junction topology is drastically modified by the proapoptotic protein tBid, to mobilize *cyt c* from the intra-cristae compartment to the IMS, before its complete release into the cytoplasm (2). How this process is controlled and related to the OMM dynamic remains unknown. OPA1 functions are involved in the fusion of the mitochondrial network, via its interaction with mitofusin (13) and the maintenance of the $\Delta\Psi_m$, and in the dynamic of cristae structure and *cyt c* release (11). 8 OPA1 isoforms result from alternate splicing of 3 exons (Ex4, Ex4b and Ex5b) (14) (Fig 1A), but their respective function is unknown. Among the almost 100 mutations, spanning the 31 exons of OPA1 (eOPA1, <http://lbbma.univ-angers.fr/lbbma.php>), that have been identified in patients affected by Autosomal Dominant Optic Atrophy (ADOA, MIM165500), none involve these 3 exons, suggesting that Ex4, Ex4b and Ex5b integrity is a strict requisite for OPA1 functions. Here, we investigate their involvement in specifying OPA1 functions.

RESULTS:

Amino acid sequence alignment between OPA1 and orthologous sequences indicated that the domain 4, corresponding to Ex4, is conserved from yeast to man, while domains 4b and 5b, corresponding to Ex4b and Ex5b, are only found in vertebrate genomes, exemplified here in mammal and fish sequences (Fig.1B) and absent from *Drosophila*, *Caenorhabditis* and lower eucaryote genomic sequences. The 17 amino-acids of the domain 4b are well conserved but do not display any specific motif or structure. The first 24 residues of the 37 amino-acid long domain 5b are highly conserved and the whole domain displays a highly conserved coiled coil structure predicted to homopolymerize (Fig.1C).

To address the function of the domains 4, 4b and 5b in mammalian cells, we compared the overexpression effects of the isoforms containing either none (OPA1-0) or one of these three domains (OPA1-4, OPA1-4b and OPA1-5b). HeLa cell cultures were transfected by vectors expressing each variant and the detection of the over-expressed OPA1 was performed by Western blotting and indirect immuno-fluorescence. In a whole cell lysate of untransfected HeLa cells, the OPA1 antibodies labeled 5 bands with different intensities ranging from 98 to 86 kDa (11) which we referred here as *a*, *b*, *c*, *d*, and *e* (Fig.2A). 24 hours after transfection, all the OPA1 isoforms were over-expressed at similar amounts and displayed one to three bands that superimposed on the endogenous forms, respectively bands *c* and *e* for OPA1-0, bands *b* and *e* for OPA1-4, band *d* for OPA1-4b, and bands *b*, *c* and *d* for OPA1-5b (Fig. 2A). The fact that overexpression of each variant, with the exception of OPA1-4b, leads to at least two peptides suggests that OPA1 is probably targeted by a second intra-mitochondrial cleavage. Mitochondrial phenotypes were observed using MitotrackerTM Red CMXRos staining and immunofluorescence (IF) using OPA1 antibody dilution that barely detect endogenous expression. Around 35% of the cells were strongly stained by IF and showed a fragmented mitochondrial networks colocalizing with the MitotrackerTM fluorescence (Figure 2C a-h). Over-expression of OPA1-0, OPA1-4 and OPA1-4b led to intermediate fragmented figures and punctuated mitochondria in almost equal proportions (Fig. 2B and 2C a-f). Cells with a low exogenous OPA1 level had mitochondria appearing as short tubules, whereas cells with high over-expression level had mitochondria appearing as dots (not shown). In addition, expression of OPA1-5b led to an homogeneous phenotype with extremely small vesicular mitochondria (Fig. 2B and 2C g,h), contrasting with the phenotype in surrounding untransfected cells (Fig. 2C, stars), or in YFP transfected cells (Fig. 2B i,j). To address the possible relationship between the mitochondrial network fission and a $\Delta\Psi_m$ dissipation, a qualitative analysis was performed using the JC-1 probe. While no $\Delta\Psi_m$ dissipation was

observed in control cells, expression of OPA1 isoforms 0, 4, or 4b, produced around 15% of cells totally devoid of red JC-1 aggregates. This value reached 30% in cultures expressing the OPA1-5b isoform. Since all cells with $\Delta\Psi_m$ dissipation displayed a punctate mitochondrial network and over-expression of OPA1 variants induced fragmentation of the mitochondrial network, we assume that the cells with $\Delta\Psi_m$ dissipation correspond to transfected cells and consequently that mitochondrial fragmentation induced by OPA1 isoform overexpression correlates with progressive $\Delta\Psi_m$ dissipation (not shown). We further examined the effect of the overexpression of OPA1 isoforms on the mitochondrial ultrastructure by TEM. HeLa cells were microinjected with a YFP or OPA1 variant expressing vectors, together with immunoglobulin conjugated to 10 nm gold beads to locate injected cells. Cells over-expressing OPA1 had predominantly small spherical mitochondria (Fig. 2D a-d), compared to the filamentous shape of mitochondria in control cells (Fig. 2D e). Nevertheless, while mitochondria of control cells or cells expressing OPA1-0, OPA1-4 or OPA1-4b showed normal cristae structure with a regular diameter (Fig. 2D a-c,e), the cristae structure of cells expressing OPA1-5b were dramatically modified, reminiscent of apoptotic mitochondria (Fig. 2D d). To assess possible apoptotic events, we used a direct DAPI labelling procedure that prevents cells detaching from the support. In HeLa cells transfected by OPA1-0, OPA1-4 and OPA1-4b or YFP, similar background levels of apoptotic like nuclei, with condensed and fragmented chromatin were observed. In contrast, 16% (+/- 4%) of cells transfected by OPA-5b, had a phenotype reminiscent of apoptosis (Fig. 3: A), that could be prevented by treating cells with the caspase inhibitor Z-VAD-fmk (data not shown). This apoptotic nuclear phenotype correlated with *cyt c* release in the cytoplasm in cells over-expressing OPA1-5b (9%, n= 200) (Fig. 3, B:j-l), while no *cyt c* release was observed in cells transfected with the other variants (Fig. 3 B:a-i) or in control cells. Thus, independently of the presence of the alternate domains, over-expression of the different OPA1 variants induced a membrane potential dissipation and fragmentation of the mitochondrial network. In addition the overexpression of OPA1-5b induced an apoptotic process with major cristae remodelling and *cyt c* release, suggesting that domain 5b function is related to the apoptotic process.

To further investigate whether special functions are associated with OPA1 domains, we selectively inhibited the expression of the endogenous OPA1 variants. 3 siRNAs, siEx4, siEx4b and siEx5b were transfected into HeLa cells, and their effects studied 72 hours later in comparison with a siRNA targeting all OPA1 variants (OPA1-siRNA) and a scramble siRNA(11). Silencing of OPA1 variants that contain the Ex4 led to the disappearance of the

most abundant OPA1 isoforms, almost as did the OPA1-siRNA. Silencing of variants containing the Ex4b led to a decrease of bands *a* and *b*, and silencing of variants containing the Ex5b led to a decrease of bands *a*, *c* and *d* (Fig. 4A). Examination of mitochondrial network morphology with MitotrackerTM Red showed that control cells had a filamentous mitochondrial network, while virtually all cells transfected with siEx4 or OPA1-siRNA showed a punctated mitochondrial network (Fig. 4B b and e). However, cells transfected with either siEx4b or siEx5b showed a highly filamentous mitochondrial network (Fig. 4B c,d) which appeared even thinner and more interconnected than in control cells (Fig 4B a). $\Delta\Psi_m$ measurement was performed by a spectroscopic quantitative approach using the JC-1 probe (Fig.4C) assessing the red to green fluorescence ratio. Significant $\Delta\Psi_m$ dissipation was observed in cells transfected with the siEx4 and this was more extensive in cells transfected with OPA1-siRNA, consistent with the fragmented mitochondrial phenotype. In cells transfected with siEx4b and siEx5b, only a slight decrease of the $\Delta\Psi_m$ was found compared to cells transfected with the scramble siRNA. Labeling chromatin with DAPI revealed that a significant proportion (Fig. 4B graph) of the cells transfected with siEx4b, siEx5b or OPA1-siRNA showed condensed and fragmented chromatin, a phenotype reminiscent of apoptotic cells (Fig. 4B f), that was absent from cells transfected with siEx4 or the scramble siRNA. To confirm that down-regulation of OPA1 variants containing Ex4b or Ex5b induced apoptosis, we assessed by Western blot the PARP cleavage, that indeed correlates with the apoptotic phenotype (Fig.4A). To further study the apoptotic process, we monitored in transfected cells (n=900) the status of the *cyt c*, using specific antibodies, and the Mitotracker dye (Fig. 5, B). In control and siEx4 transfected cells, *cyt c* IF perfectly colocalized with the Mitotracker fluorescence in mitochondria. In siEx4b and siEx5b transfected cultures, some cells (6%) showed partial release of *cyt c* (phenotype a) with the mitochondrial network still highly tubular. Very few cells (< 0.5%) showed a complete release of *cyt c* and Mitotracker fluorescence into mitochondria (phenotype b). In addition, we evidenced cells (>2%) with a uniform cytoplasmic *cyt c* fluorescence and an unusual uniform cytoplasmic Mitotracker fluorescence (phenotype c), suggesting that in these cells the membrane potential was beyond the minimal level required for the Mitotracker to accumulate into mitochondria. In cells treated with the OPA1-siRNA, a significant proportion showed a partial (7%) or complete (22%) release of *cyt c*, with a uniform Mitotracker fluorescence in the mitochondrial network. Finally, we explored the mitochondrial ultrastructures by TEM (Fig. 4Bg-k). Consistent with former observations, mitochondrial shapes were tubular for control cells and siEx4b and

siEx5b transfected cells (Fig.4B g,i,j), and spherical in siEx4 and OPA1-siRNA transfected cells (Fig. 4B h,k). Surprisingly, no major perturbations of the IMM structure, and in particular of the cristae morphology, were observed in cells transfected by the exon specific siRNAs or in control cells (Fig. 4B g-j), in contrast to cells transfected by the OPA1-siRNA (Fig. 4B k).

DISCUSSION:

OPA1-Ex4 involvement in mitochondrial dynamic.

Taking together our results on the mitochondrial network dynamics, we observed that OPA1 variant over-expression induced fission of the mitochondrial network, as the silencing of OPA1 variants containing the Ex4. This suggests that modifying OPA1 abundance interferes with its basic functions, that consist in $\Delta\Psi_m$ maintenance and membrane fusion. Conversely, results from silencing of Ex4b and Ex5b suggest that domain 4b or 5b do not interfere with the fusion process or the membrane potential. Therefore, the presence of domain 4 in OPA1, which is conserved in all OPA1 ortholog sequences, specifies functions associated with the $\Delta\Psi_m$ maintenance and fusion of the mitochondrial network, that are conserved throughout evolution, as similar observations were found in yeasts (15; 16).

OPA1-Ex4b or 5b involvement in the apoptotic process.

Our results from OPA1-5b overexpression and Ex4b and Ex5b silencing evidenced two types of apoptotic processes based on *cyt c* release. The first one, already described for the silencing of all OPA1 isoforms, is similar to that found for overexpression of OPA1-5b and corresponds to most apoptotic processes described in the literature. Cells undergo mitochondrial fission, $\Delta\Psi_m$ dissipation, cytoplasm shrinkage, major modifications of the cristae structure and rapid and complete *cyt c* release to terminate with nuclear fragmentation. The second form of apoptosis was observed when OPA1 variants containing Ex4b or Ex5b were silenced. In these later cases, cells undergo apoptosis without mitochondrial network fission, without major $\Delta\Psi_m$ dissipation, with very few cells showing complete *cyt c* release and without major modifications of the cristae structure. These observations suggest that a discrete modifications of the IMM, undetectable by conventional TEM, are sufficient for a progressive, probably slow process of *cyt c* mobilization and release, that do not affect other processes associated with IMM integrity. The uncoupling of this apoptotic process from mitochondrial network fission and the presence of some cells showing complete *cyt c* release with an unusual cytoplasmic Mitotracker dye staining, suggest that the final $\Delta\Psi_m$ dissipation is not associated with an apoptotic specific process, but probably to the *cyt c* progressive release and subsequent impairment of the respiratory chain.

Since the absence of both domains 4b and 5b led to this apoptotic process, one might speculate that OPA1 isoforms including these domains have a specific and restricted function in trapping *cyt c* inside mitochondria and in particular within cristae. Because cristae junction

remodelling, *cyt c* release during apoptosis and alternate splicing in OPA1 have only been described in vertebrates (12); (17), we propose that these processes result from co-evolution and constitute a vertebrate specific mechanism controlling segregation of *cyt c*. Domain 5b that is predicted to form a homo-polymerizing coiled-coil structure, might induce a higher level of OPA1 assembly to form a tight structure “plugging” cristae junction. Its absence would mobilize *cyt c* into the IMS and allow subsequent release into the cytoplasm, without initial modification of other mitochondrial functions. Similarly, domain 4b could positively regulate this complex structure and consequently, its absence would generate a similar process leading to *cyt c* release.

Mitochondrial fate associated to OPA1 alternate splicing.

Our data suggest that mitochondrial fusion and susceptibility to apoptosis might be basically regulated by the splicing machinery and consequently that the relative abundance of each OPA1 isoform can contribute to adapt mitochondrial dynamic to cell types and growth conditions. In this respect, characterization of the expression levels of each variant in human retinal ganglion cells might contribute to identify the patho-physiological mechanism responsible for their susceptibility to degeneration in optic neuropathies.

MATERIAL AND METHODS.

Antibodies.

OPA1 antibodies were as previously described (6). Commercial antibodies were from the sources indicated: monoclonal anti-cytochrome c (Promega), polyclonal anti-cleaved PARP (Promega), monoclonal anti actin (Chemicon), Alexa-594 anti-rabbit IgG and Alexa-488 anti-mouse IgG (Molecular Probes), anti-rabbit IgG-HRP and anti-mouse IgG-HRP (New England Biolabs).

Cell culture, plasmid transfection and Western blots.

HeLa cells were cultured in DMEM, 10% FCS, 5 % CO₂. OPA1 variants were cloned by RT-PCR using oligonucleotides situated in the exons 3 and 5 to amplify sequences either containing or not exons 4 and 4b, and oligonucleotides situated in exons 5 and 9 to amplify sequences either containing or not exon 5b. All amplified fragments were cloned in the topo-pCRII vector (Invitrogen), sequenced, and recombined in OPA1 open reading frame to provide the 4 transcripts. They were further sub-cloned in the pCCEY plasmids. SiRNA (Dharmacon Research) experiments were carried out as described previously with some modifications (11; 18). The sequences of the regions targeted by the siEx4, siEx4b and siEx5b are respectively 5'-AAGATTGTTGAAAGCCTTAGCTT-3', 5'-AAGTCATAGGAGCTTCTGACCTA-3', and 5'-AAGAGGAAGCGCGCAGAGCCGCT-3'. Final concentration of the siRNA duplex in culture medium was 100 nM. Transfections of HeLa cells were performed with Lipofectamine 2000® reagent (Invitrogen). Inhibition of caspases was performed with 100µM z-VAD-fmk (Calbiochem). To detect OPA1 and actin by Western blots, transfected cells were harvested, washed once in PBS and equal amounts of proteins were solubilized in 50µl Laemmli sample buffer and boiled for 10 minutes. Samples were run on 7% polyacrylamide gels and transferred to nitrocellulose. Immuno-detection (anti-OPA1: 1/2000 for over-expression experiments and 1/400 for RNAi; anti-actin: 1/10000; IgG-HRP: 1/10,000) was carried out using ECL (Amersham Pharmacia Biotech). PARP detection was performed according to the protocol from Promega (anti-PARP: 1/400).

Microscopy.

For indirect immunofluorescent microscopy, cells grown on glass coverslips were fixed in PBS, 3.7% paraformaldehyde (30 min, 4°C), permeabilized in PBS, 0.2% Triton X-100 (10 min, room temperature) and immuno-labelled in PBS, 2% BSA, using the following antibodies (OPA1: 1/800; cyt c: 1/1000; Alexa-594 anti-rabbit IgG: 1/600; Alexa-488 anti-mouse IgG: 1/600) and stained with DAPI (0.1µg/ml). For the cyt c localisation in siRNA transfected cells, phenotypes were counted on 300 cells in duplicate experiments. For direct

labelling procedure of mitochondria and chromatin, cell cultures were stained using 100nM CMXros Mitotracker® Red (Molecular Probes) for 30 minutes, then fixed and DAPI stained. To analyze the $\Delta\Psi_m$, cells were incubated 20 minutes with 5 μ g/ml JC-1 (Molecular Probes) in culture medium and either directly observed in microscopy in culture medium without phenol red (GIBCO), or subsequently collected, washed in PBS, and processed for fluorescence analysis on an Ascent Fluoroscan using the Ascent Software (excitation 488nm; emission 538 nm and 590 nm). The ratio of the fluorescence at 590 nm, proportional to the $\Delta\Psi_m$, to that at 538 nm, proportional to the mass of mitochondria, was calculated from triplicate values obtained in the course of three independent experiments. Fluorescence images were acquired and processed using a Leica DMIRE-2 microscope.

For TEM, cells were either transfected by siRNA and analysed 72 hours afterwards, or micro-injected using a Zeiss Axiovert microinjector with the different plasmids in the presence anti-rabbit antibodies conjugated to 10 nm gold beads (EMS) and harvested after 24 hours. Cells were fixed for 2 hours with 4% glutaraldehyde in sodium cacodylate buffer, post-fixed for 1h with 1% osmium tetroxide, dehydrated and embedded in Epon (EMS). Thin sections collected onto nickel grids were stained with 1% uranyl acetate and 0.3% lead citrate, and observed in a JEOL-1200 EX electron microscope at 80 kV.

ACKNOWLEDGEMENTS:

We are indebted to the IFR 109 and to Nacer Benmérâgui for technical help in electron microscopy, to Martine Cazales for technical help for microinjections, to Keith Langley for comments on the manuscript and to members of the UMR5088 and INSERM U583 for helpful discussions. Work was supported by grants from CNRS, INSERM, Rétina France, FRM, Fondation Electricité de France and l'AFM. A.O. was a recipient of an ARC fellowship.

Reference List

1. Perfettini, J.L., Roumier, T. and Kroemer, G. Mitochondrial fusion and fission in the control of apoptosis. *Trends Cell Biol* 15:179-83, 2005.
2. Scorrano, L., Ashiya, M., Buttle, K., et al. A distinct pathway remodels mitochondrial cristae and mobilizes cytochrome c during apoptosis. *Dev Cell* 2:55-67, 2002.
3. Santel, A. and Fuller, M.T. Control of mitochondrial morphology by a human mitofusin. *J Cell Sci* 114:867-74, 2001.
4. Eura, Y., Ishihara, N., Yokota, S. and Mihara, K. Two mitofusin proteins, mammalian homologues of FZO, with distinct functions are both required for mitochondrial fusion. *J Biochem (Tokyo)* 134:333-44, 2003.
5. Smirnova, E., Griparic, L., Shurland, D.L. and van der Bliek, A.M. Dynamin-related protein Drp1 is required for mitochondrial division in mammalian cells. *Mol Biol Cell* 12:2245-56, 2001.
6. Olichon, A., Emorine, L.J., Descoins, E., et al. The human dynamin-related protein OPA1 is anchored to the mitochondrial inner membrane facing the inter-membrane space. *FEBS Lett* 523:171-6, 2002.
7. Karbowski, M., Lee, Y.J., Gaume, B., et al. Spatial and temporal association of Bax with mitochondrial fission sites, Drp1, and Mfn2 during apoptosis. *J Cell Biol* 159:931-8, 2002.
8. Lee, Y.J., Jeong, S.Y., Karbowski, M., Smith, C.L. and Youle, R.J. Roles of the mammalian mitochondrial fission and fusion mediators Fis1, Drp1, and Opa1 in apoptosis. *Mol Biol Cell* 15:5001-11, 2004.
9. Germain, M., Mathai, J.P., McBride, H.M. and Shore, G.C. Endoplasmic reticulum BIK initiates DRP1-regulated remodelling of mitochondrial cristae during apoptosis. *EMBO J* 2005.
10. Legros, F., Lombes, A., Frachon, P. and Rojo, M. Mitochondrial fusion in human cells is efficient, requires the inner membrane potential, and is mediated by mitofusins. *Mol Biol Cell* 13:4343-54, 2002.
11. Olichon, A., Baricault, L., Gas, N., et al. Loss of OPA1 perturbs the mitochondrial inner membrane structure and integrity, leading to cytochrome c release and apoptosis. *J Biol Chem* 278:7743-6, 2003.
12. Frey, T.G. and Mannella, C.A. The internal structure of mitochondria. *Trends Biochem Sci* 25:319-24, 2000.

13. Cipolat, S., Martins de Brito, O., Dal Zilio, B. and Scorrano, L. OPA1 requires mitofusin 1 to promote mitochondrial fusion. *Proc Natl Acad Sci U S A* 101:15927-32, 2004.
14. Delettre, C., Griffoin, J.M., Kaplan, J., et al. Mutation spectrum and splicing variants in the OPA1 gene. *Hum Genet* 109:584-91, 2001.
15. Wong, E.D., Wagner, J.A., Scott, S.V., et al. The intramitochondrial dynamin-related GTPase, Mgm1p, is a component of a protein complex that mediates mitochondrial fusion. *J Cell Biol* 160:303-11, 2003.
16. Guillou, E., Bousquet, C., Daloyau, M., Emorine, L.J. and Belenguer, P. Msp1p is an intermembrane space dynamin-related protein that mediates mitochondrial fusion in a Dnm1p-dependent manner in *S. pombe*. *FEBS Lett* 579:1109-16, 2005.
17. Kornbluth, S. and White, K. Apoptosis in *Drosophila*: neither fish nor fowl (nor man, nor worm). *J Cell Sci* 118:1779-87, 2005.
18. Elbashir, S.M., Harborth, J., Weber, K. and Tuschl, T. Analysis of gene function in somatic mammalian cells using small interfering RNAs. *Methods* 26:199-213, 2002.

TITLES AND LEGENDS TO THE FIGURES:

Figure 1. (A) Schematic representation of human OPA1 variants

Schematic representation of primary structures of the 8 OPA1 variants and the precursor predicted molecular weight. Arrows indicates predicted mitochondrial pre-sequence cleavage sites. mRNA isoform numbering corresponds to PubMed classification (B) **Evolutionary conservation of domain 4b and 5b.** Amino-acid alignment of the domains 4b and 5b. *Hs: homo sapiens, Rt: Ratus norvegicus Mm: mus musculus, Dr: Danio rerio , Fr: Fugu rubripes.* (C) Probability of coiled-coil structure for domain 5b in man and Fugu.

Figure 2. OPA1 variant over-expression in HeLa cells induces fragmentation of the mitochondrial network and a loss of $\Delta\Psi_m$.

HeLa cells were transfected with plasmids expressing OPA1-0, OPA1-4, OPA1-4b, OPA1-5b, or control plasmids expressing YFP or nothing (mock) and processed 24 hours after transfection. (A) Western blot analyses of whole cell extracts probed with anti-OPA1 (1/2000) or anti-actin (1/10000) antibodies. Endogenous OPA1 signal is shown in mock transfected cells. Actin labelling was used as a loading control (B) Percentage of phenotypes shown above the table, among transfected cells. (C) Mitotracker® Red and DAPI staining (a, c, e, g, i) and immuno-fluorescence anti-OPA1 labelling (b, d, f, h, j) fluorescence in transfected cells. Untransfected cells are shown by stars. (D) TEM micrographs of thin section of HeLa cells showing the ultrastructure of mitochondria 24 h after microinjection of plasmids. Bars 100 nm.

Figure 3. Cytochrome c release correlates with OPA1-5b induced apoptosis. HeLa cells were transfected with plasmids expressing OPA1-0, OPA1-4, OPA1-4b, OPA1-5b and processed 24 hours after transfection. (A) Quantification of apoptotic nuclei with DAPI staining. (B) Cells, treated with Z-VAD-fmk (100 μ M) 4 hours after transfection, were fixed at 24 h, stained with DAPI, and immuno-labelled with anti-OPA1 (1/800) (red: a, d, g, j,) and anti-cytochrome c (green: b, e, h, k.). Merged (c, f, i, l.). Untransfected cells are shown by stars.

Figure 4. Exon specific siRNA uncouples functions in mitochondrial network fusion and apoptosis.

HeLa cells were transfected with siRNA matching the alternatively spliced exons, siEx4, siEx4b and siEx5b, or with the OPA1-siRNA or with the scramble as controls, and processed 72 hours after transfection. **(A)** Western blot analyses of whole cell extracts, probed with anti-OPA1 (1/400) or anti-actin (1/10000) antibodies. **(B)** Analysis of Mitotracker® Red and DAPI staining by fluorescence microscopy (a-f). Percentage cells showing a filamentous or punctate mitochondrial network, or showing an apoptotic phenotype (graph). Transmission electron microscope micrographs of thin section of HeLa cells showing the ultrastructure of mitochondria (g-k). Bars 100 nm **(C)** $\Delta\Psi_m$ assesment using JC-1 dye.

Figure 5. Assesment of cytochrome c release in cells transfected by the different siRNAs.

HeLa cells were transfected by the 5 different siRNA, then processed after 72 hours for cytochrome c IF and Mitotracker® Red fluorescence and DAPI staining. **(A)**: phenotypes observed : - a: *cyt c* partially released in the cytoplasm; - b: *cyt c* completely released in the cytoplasm and mitochondrial Mitotracker labelling; - c: *cyt c* completely released in the cytoplasm and cytoplasmic Mitotracker florescence. **(B)**: Relative amounts of the 3 phenotypes in the siRNA transfected cultures (n=900).

RNA forms*	protein isoforms							predicted M. W. kDa				
2	OPA1-0	N	mts	TM	CC	GTPase domain	CC	C	108			
3	OPA1-4	N	mts	TM	4	CC	GTPase domain	CC	C	109		
1	OPA1-4b	N	mts	TM	4b	CC	GTPase domain	CC	C	112		
4	OPA1-5b	N	mts	TM	5b	CC	GTPase domain	CC	C	112		
5	OPA1-4.4b	N	mts	TM	4	4b	CC	GTPase domain	CC	C	114	
7	OPA1-4.5b	N	mts	TM	4	5b	CC	GTPase domain	CC	C	114	
6	OPA1-4b.5b	N	mts	TM	4b	5b	CC	GTPase domain	CC	C	116	
8	OPA1-4.4b.5b	N	mts	TM	4	4b	5b	CC	GTPase domain	CC	C	118

Domain 4b

H.s. HKLVSEVIGASDLLLLL
M.m. PKLVSEVLEVSEALLLL
R.n. PKLVSEVIEASEPLLLL
D.r. TGLGSEVNGASGLRLLL
F.r. VSLVSEVKGASGLHLLL

Domain 5b

H.s. GLLGELILLQQQIQEHEEEARRAAGQYSTSYAQQKRK
M.m. GLLGELILLQQQIQEHEEEARRAAGQYSTSYAQQKRK
R.n. GLLGELILLQQQIQEHEEEARRAAGQYSTSYAQQKRK
D.r. GLLSELIVIQQQIQEHEEEMRRAAA-NNAPPPPRDPS
F.r. GLLGELILIQQQIQEHEEEVRRAAAANNARPPPEPA

C

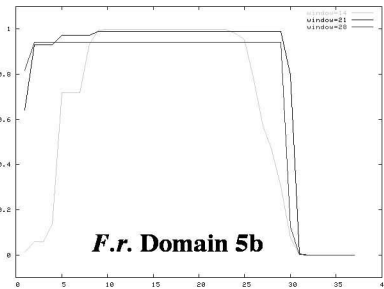
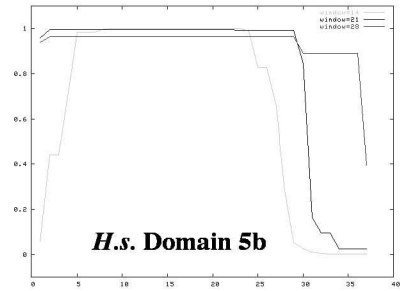
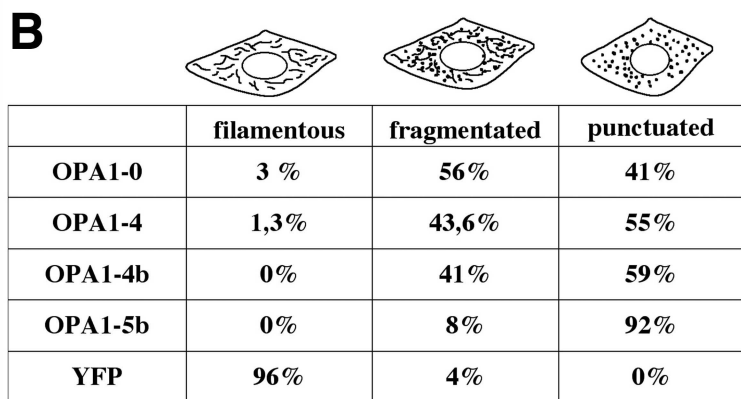
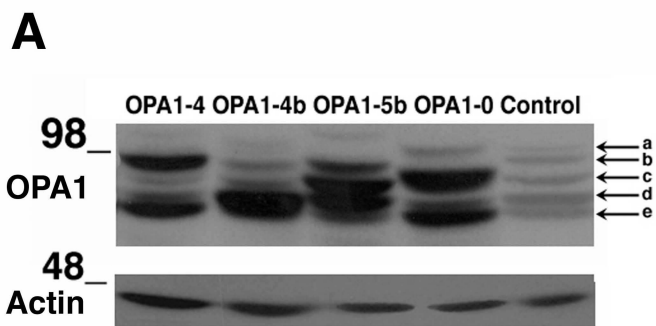
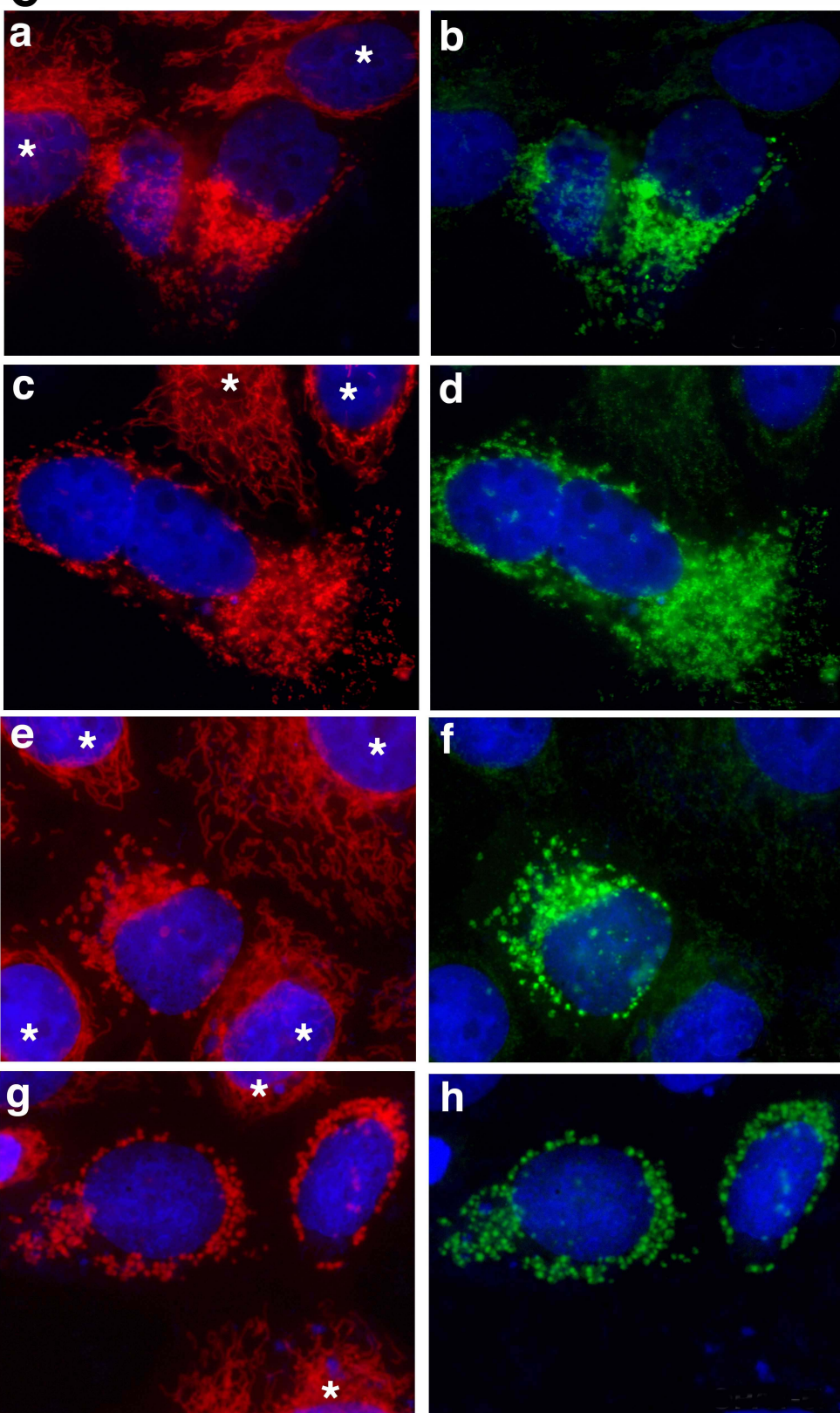


Figure 1, Olichon et al.

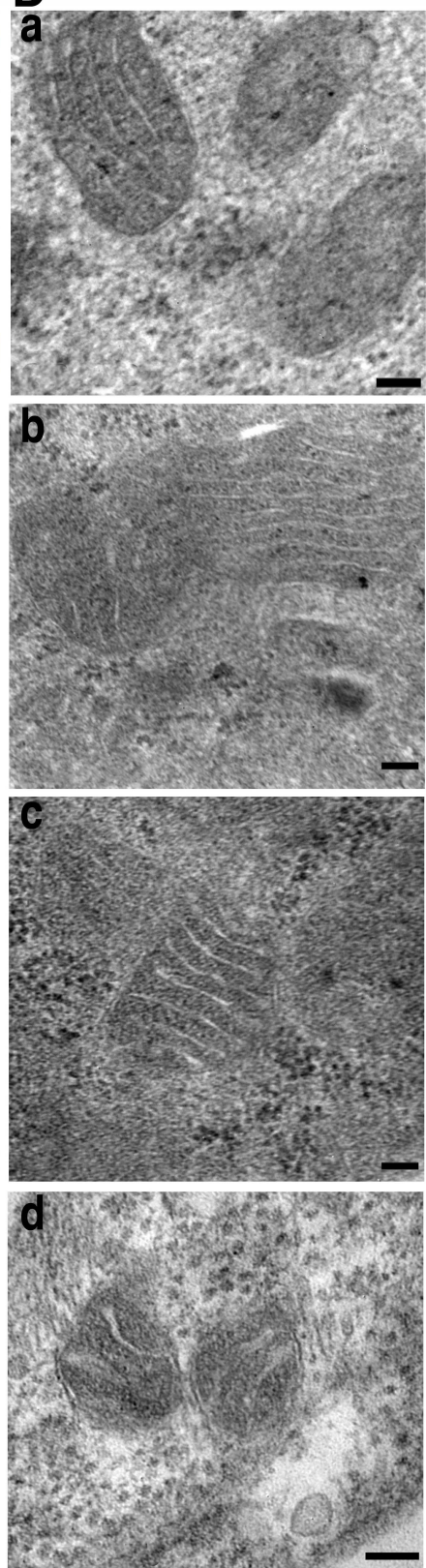


C Mitotracker + DAPI

OPA1



D



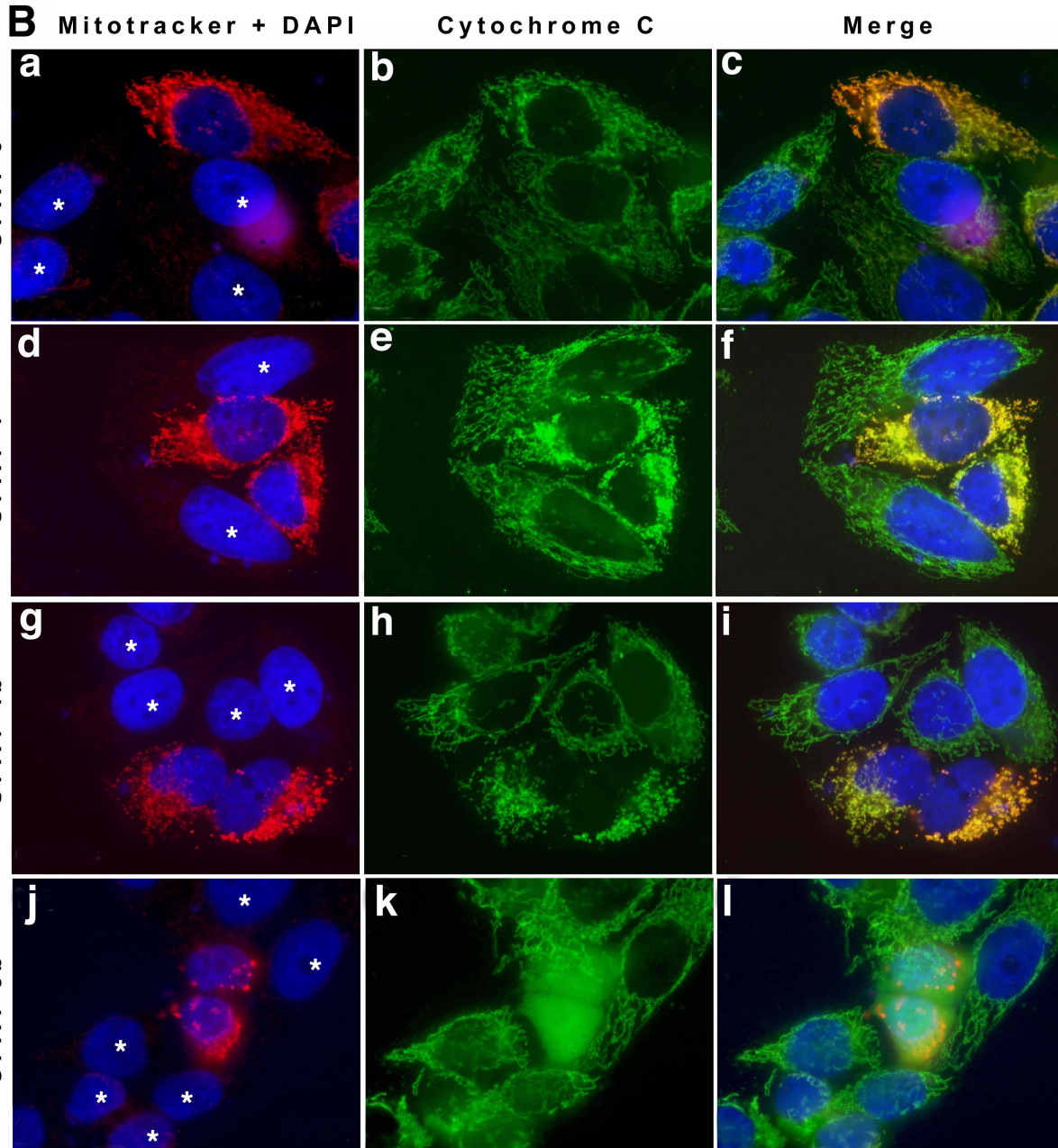
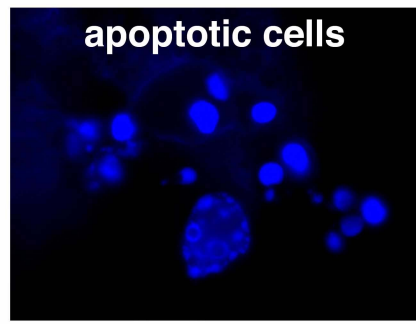
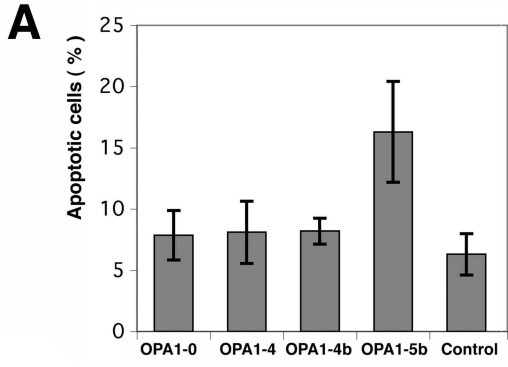


Figure 3, Olichon et al.

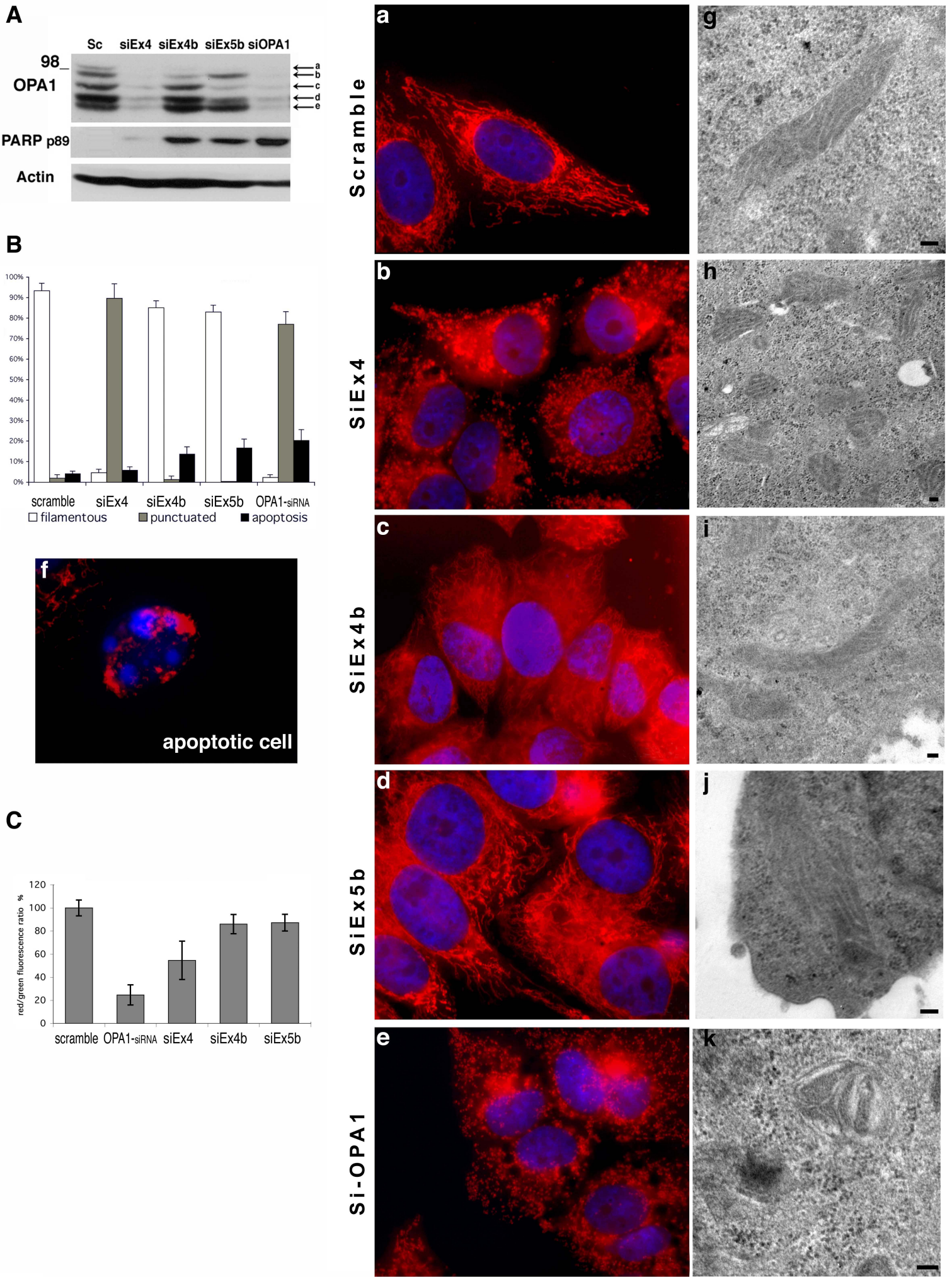


Figure 4, Olichon et al.

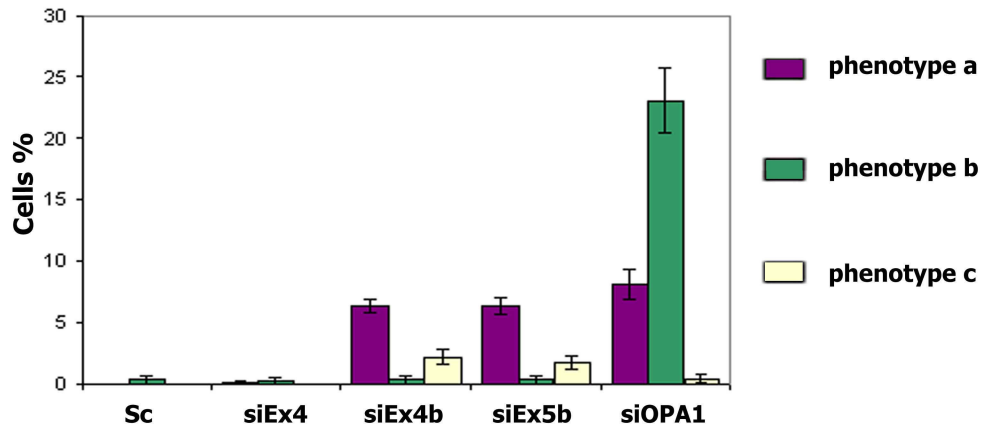
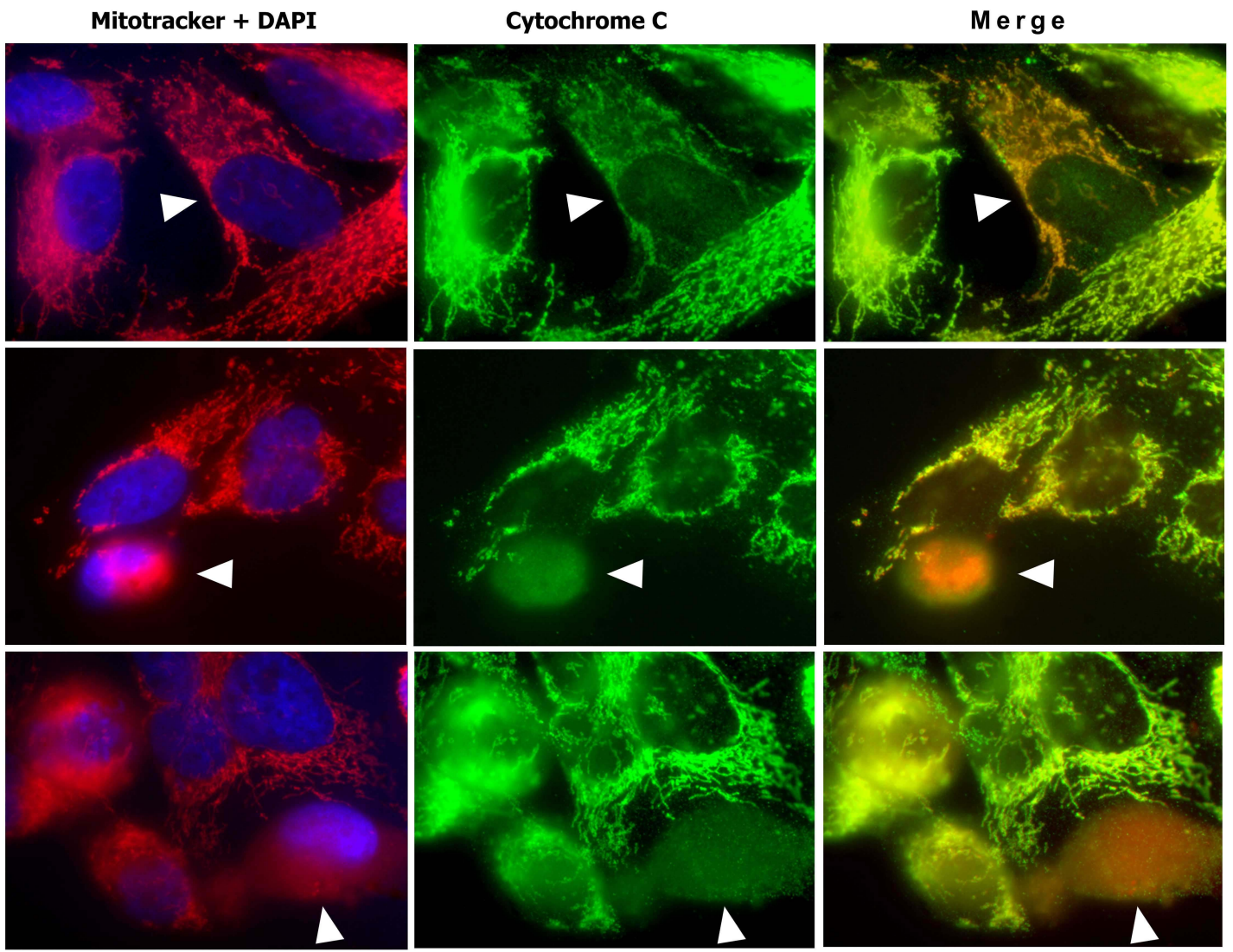


Figure 5, Olichon et al.